Coastal Engineering 197 (2025) 104689

Contents lists available at ScienceDirect

Coastal Engineering

journal homepage: www.elsevier.com/locate/coastaleng

New 2D laboratory experiments on wave overtopping at vertical walls under impulsive and non-impulsive conditions

Claudia Cecioni [a,*], Yuri Pepi [b], Leopoldo Franco [a]

[a] Department of Civil, Computer Science and Aeronautical Technologies Engineering, Roma Tre University, Rome, Italy
[b] Department of Civil Engineering, Ghent University, Ghent, Belgium

ARTICLE INFO

Keywords:
Mean overtopping discharge
Individual overtopping volumes
Vertical structures
Gentle foreshore
Physical model

ABSTRACT

This paper describes 2D physical model study on wave overtopping at vertical coastal structures. Results of two experimental campaigns are presented, where different wave and geometrical parameters are considered. Wide ranges of relative water depth at the toe of the structure and relative crest freeboard are explored, considering two foreshore slopes in front of the vertical wall. Wave–wall interactions both for pulsating and impulsive regime are tested. The wave overtopping time series measurement allows to analyze not only mean overtopping discharges but also individual overtopping volumes. Single overtopping volumes distribution is investigated relating it to geometrical and hydraulic parameters.

The present experimental analysis is coherent with the literature, in the already explored range of wave and geometrical parameters of the structure; moreover, it extends the previous findings, providing two main outcomes: (i) new mean wave overtopping measurements for a wider ranges of relative water depth and relative freeboards; (ii) new individual wave overtopping volumes measurements at vertical walls, specifically under impulsive conditions. New insights on the mean overtopping discharge and on the probability distribution of individual overtopping volumes are provided.

1. Introduction

Vertical coastal structures expose a plain vertical or quite steep face to the sea side and are designed to protect harbors or coastal areas. These structures can be fronted by relatively deep water and in these cases they are typically built with sand-filled concrete caisson breakwaters, or they can be placed in shallower water, mainly seawalls or bulkheads.

For a safe design, vertical structures should limit wave induced overtopping hazard and protect people and/or activities behind the crest of the structure itself. The prediction of overtopping has based historically on estimating the mean overtopping discharge, q (in m^3/s per meter structure width). Results of physical models and in situ measurements allowed the scientific community to mostly develop empirical formulae (Owen, 1980; Van der Meer and Janssen, 1994; Goda, 2009; EurOtop, 2007, 2018; Etemad-Shahidi et al., 2016; Shaeri and Etemad-Shahidi, 2021; Gallach-Sánchez et al., 2021), graphical methods (Goda et al., 1975; Herbert, 1993) and machine learning techniques (Van Gent et al., 2007; Zanuttigh et al., 2016; den Bieman et al., 2021) to determine average overtopping discharge at coastal structures. Some numerical models have also been developed to reproduce overtopping flow in wave flumes or basins (Hu et al., 2000; Losada et al., 2008; Akbari, 2017; Suzuki et al., 2017; Lashley et al., 2021). Guidance manuals were published in various countries (AW, 2002; EAK, 2002; Besley, 1999; USACE, 2002) to provide guidelines on wave overtopping and run-up.

Within the European funded project CLASH (De Rouck et al., 2009), the reliability of wave overtopping prediction has improved and the European Manual for the Assessment of Wave Overtopping manual (EurOtop, 2007) has been published, based on the analysis of more that 10,000 irregular wave overtopping tests, (Van der Meer et al., 2009). Further studies (Victor and Troch, 2013; Van der Meer and Bruce, 2014) have led to an improvement of overtopping formulae and a new version of the EurOtop manual has been released (EurOtop, 2018).

Although most of the literature has investigated mean overtopping rates, studies that focus specifically on wave-by-wave overtopping analysis are increasing, but still remain more limited. Indeed, field and experimental observations demonstrate the need of considering, for a safe design of a coastal structures, not only the mean discharge but also other parameters, as the individual maximum overtopping volume (V_{max}), the probability distribution of individual wave overtopping volumes, the overtopping flow velocity and its thickness over the crest. The first studies on wave overtopping in a wave-by-wave form are

* Corresponding author.
E-mail address: claudia.cecioni@uniroma3.it (C. Cecioni).

https://doi.org/10.1016/j.coastaleng.2024.104689
Received 19 July 2024; Received in revised form 29 November 2024; Accepted 12 December 2024
Available online 18 December 2024

from Van der Meer and Janssen (1994) for sloping defense structures and Franco et al. (1994) for vertical walls in relatively deep water. The authors found that the two-parameter Weibull distribution gives a very good fit of the exceeding probability with the single volumes overtopping data. Although a larger bibliography exists for individual overtopping over sloping structures, more limited studies exist for vertical structures (Besley, 1999; Franco and Franco, 1999; Pearson et al., 2003; Bruce et al., 2010; Victor et al., 2012; Salauddin and Pearson, 2019; Salauddin et al., 2022).

Two different overtopping responses, and also wave forces responses, can be clearly identified, depending on the wave-structure interaction regimes: (i) in relatively deep water, incoming waves are reflected without breaking by the vertical structure, and they induce pulsating, or non-impulsive, wave forces and overtopping; (ii) in shallow waters, on the contrary, incoming waves break at the toe of the structure, inducing impulsive loads and overtopping.

Impulsive wave overtopping is a complex and crucial phenomenon in coastal engineering, significantly impacting the design, maintenance and performance of vertical structures. Gentle foreshores in combination with shallow water conditions lead to heavy wave breaking and a significant change of the wave spectra from offshore to the toe of the structure, moving energy from the higher to the lower frequencies. The wave conditions at the toe of a structure in case of shallow foreshore are known to be dominated by low frequency waves, and the spectral significant wave height and the spectral period change drastically from those at offshore condition. These two parameters indeed, significantly influence wave overtopping, as demonstrated experimentally (Van Gent and Smith, 1999; Altomare et al., 2016; Briganti et al., 2022). For instance, when the relative water depth, h_t/H_{m0}, (with h_t the water depth at the toe of the structure and H_{m0} the significant incident wave height) is smaller than 1, the spectral period, $T_{m-1,0}$, can be more than 5 times larger than in deep water, depending on the foreshore slope (Hofland et al., 2017).

The wave overtopping under impulsive conditions was investigated within the VOWS (Violent Overtopping of Waves at Seawalls) project, including new laboratory experiments and prototype measurements. The goal of this project was to provide guidelines for predicting processes at prototype scale (Pearson et al., 2003), emphasizing the importance of considering scale effects when reproducing laboratory tests under impulsive conditions. Further studies have been recently conducted and are ongoing among the authors of Franco et al. (2022), within the WOW project (Wave Overtopping at Walls). In particular, Franco et al. (2022) presented the preliminary results of two experimental campaigns: one performed at the wave flume of Edinburgh University (Scotland, UK), where a vertical wave wall over a foreshore 1:10 sloped was modeled, another performed at the wave flume of Roma Tre University (Rome, Italy), with a vertical wave wall over a foreshore 1:50 sloped.

Furthermore, within WOW, new 2D physical model tests have been carried out at Roma Tre University laboratory (UR3), and others are planned at Edinburgh University. The new tests of UR3 extend the study to vertical wall facing to an horizontal foreshore, with a wider range of water depths.

The present paper analyzes the experimental data from both campaigns carried out at UR3 wave flume, within the WOW project. The physical models have been performed with the aim of analyzing wave overtopping both in non-impulsive and impulsive conditions. The main motivations were twofold: to measure mean overtopping discharge at vertical walls in range not yet fully explored, and to measure individual wave overtopping at vertical walls. Specifically, the present experimental tests (i) provide mean overtopping discharge for horizontal and 1:50 sloped foreshore; (ii) extend (Goda, 2010; EurOtop, 2018) results for violent overtopping at relative freeboards higher than 2 and 3.3 respectively; (iii) perform tests with large relative water depth for non-impulsive condition. Regarding point (ii) the relative freeboard has been increased up to the condition when no overtopping is measured, or when mean overtopping discharge is less than 10^{-6} $m^3/s/m$. Moreover, measurements of individual overtopping volumes at vertical walls allow to fill some gaps in the literature, especially for impulsive conditions.

The paper is structured as follows: next section describes the experimental campaigns carried out, at Roma Tre University wave flume; in the following section laboratory results are analyzed, making distinction between non-impulsive and impulsive wave/structure interaction's regime and considering mean overtopping discharge, maximum volume and wave volumes distribution, including a comparison with the existing predictive formulae; then conclusions are given.

2. Experimental setup

2.1. Wave flume

The experiments have been carried out at the hydraulics laboratory of the Engineering Department of Roma Tre University (Rome, Italy). The facility is equipped with a wave flume which is 20.0 m long, 0.6 m wide and 1.0 m high. The side walls of the flume are made of glass and steel. A piston-type wave maker (maximum stroke equal to 1.35 m) is able to generate both regular and irregular waves in the flume. The wave generation system is controlled by the state-of-the-art software AWASYS 7 (Aalborg University, www.hydrosoft.civil.aau.dk/awasys), including an Active Wave Absorption System (Andersen et al., 2017, 2018). The flume is equipped with resistive wave gauges (VTI Resistive Wave Gauge Modules installed in a WG-16CH rack) to measure the free surface elevation and perform the analysis of separation between incident and reflected wave. Two wave gauges were always placed on the wave paddle and are used for the active wave absorption. The acquisition frequency of the wave gauges is 50 Hz. The wave gauges were calibrated at least twice daily or when the water level has been changed, to account for possible differences through the day in the laboratory environment (Hughes, 1993).

2.2. The two experimental campaigns

Two experimental campaigns have been carried out in the same wave flume. Both are intended to reproduce wave interaction with a plain vertical wall, with the final goal of measuring wave overtopping volumes and mean discharge. During one experimental campaign, waves are generated and propagated over a constant water depth, for brevity now named HB (Horizontal Bottom) configuration; while in the other campaign a 1:50 sloping foreshore is reproduced in front of the vertical wall; these experimental tests are named SF (Sloping Foreshore).

The longitudinal view of the wave flume with the two model setups is schematized in Fig. 1. Here wave gauges are named with capital letters and their positions are reported in meters from one end of the flume. Please note that gauges F, G and H in the SF configuration were placed only in preliminary calibration tests, carried out without the wall as explained later in Section 2.5, at a relative distance of 0.2 m. For the SF configuration, the transition from the 1:50 slope and the horizontal bottom of the flume was made with a steeper slope (1:20). The foreshore consists of a hard top layer of concrete placed on a bottom layer of wood panel over a steel structure. This foreshore guarantees a fixed difference of 0.41 m between the water depth in front of the wave-maker and that at the toe of the vertical wall.

2.3. Wave overtopping measurements

The measurements of overtopping discharge and wave-by-wave volumes were taken with two different methods in the two campaigns. In the HB tests (see pictures in Fig. 2) an overtopping tank was fixed inside the flume behind the wall to record the overtopping water by means of a resistive gauge inside the tank itself (wave gauge F in Fig. 1,

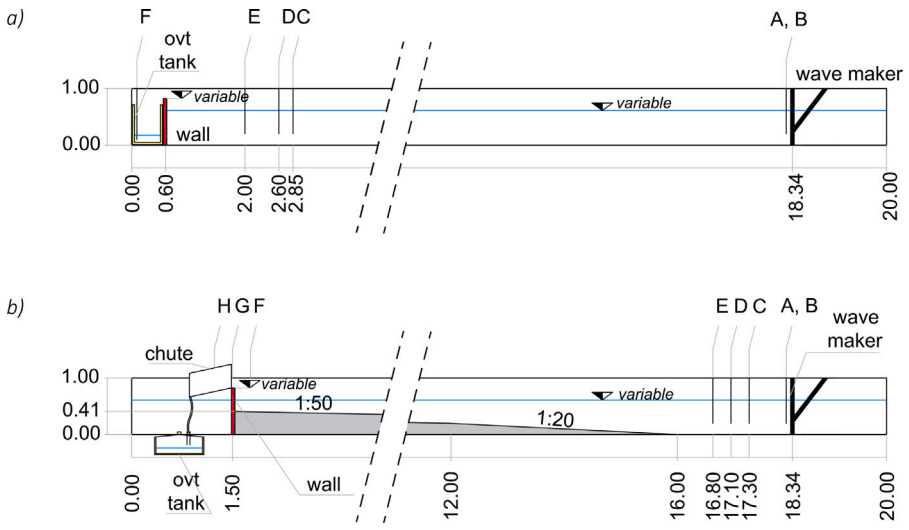

Fig. 1. Cross sections of wave flume for HB configuration (a) and SF configuration (b), with location of gauges named A to H.

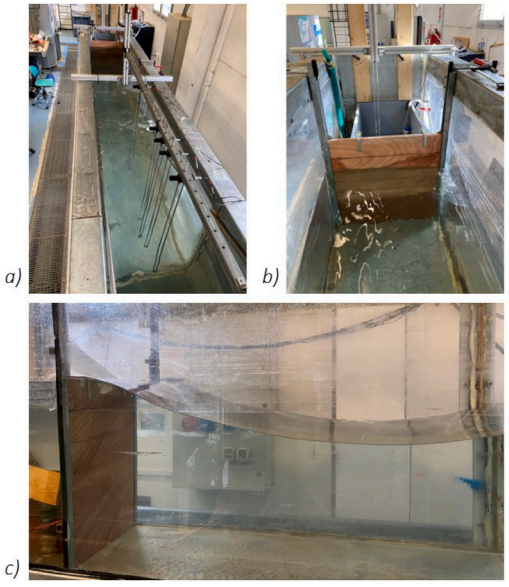

Fig. 2. Pictures during HB tests: (a) view of the wave flume, wave gauges and vertical wall at the end; (b) view of the wall with the overtopping tank behind it; (c) pulsating wave impact on the wall.

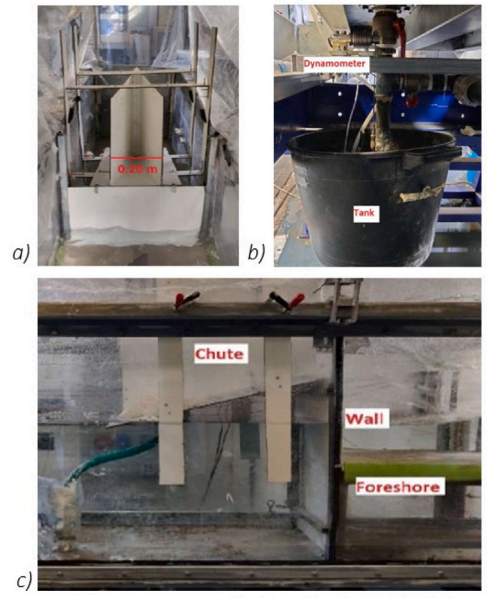

Fig. 3. Pictures during SF tests: (a) front view of the vertical wall and the overtopping chute behind it; (b) view of the overtopping tank below the wave flume; (c) lateral view of the flume, with foreshore, wall and overtopping chute.

panel (a)). The acquisition frequency was 50 Hz as for the wave gauges inside the flume. The overtopping tank has a width of 0.38 m and it is placed centered with respect of the 0.60 m wide wall to minimize any side effects.

In the SF configuration, as shown in Fig. 1(b) and from the pictures of Fig. 3, a chute collected the overtopping water in a tank located below the wave flume. The width of the chute was 0.20 m, again placed at the center of the wall. The tank was equipped with a dynamo-meter, with a 2000 Hz acquisition system and an accuracy that allowed for detection of differences in volume of less than 0.001 l (or 1 g).

A pump was installed in the overtopping tanks in both experimental campaigns, to empty the tanks when the water level reached a certain point. The water was pumped back from the tank into the wave flume behind the structure, in order to avoid disturbing the wave field.

2.4. Test program

Table 1 summarizes the water level and wave conditions tested in both experimental campaigns, where Θ represents the foreshore slope, h_t is the water depth at the toe of the vertical wall, R_c is the wall crest freeboard. The significant wave height H_{m0}, the wave steepness $s_{m-1,0}$ and the spectral wave period $T_{m-1,0}$ are reported in Table 1. For the SF tests, these wave parameters values are reported both in the offshore position, i.e. in front of the wave-maker, and at the toe of the vertical wall (the subscripts o and t stand respectively for offshore and at the toe of the structure). The wave steepness, $s_{m-1,0}$ is calculated as $H_{m0}/L_{m-1,0}$, with $L_{m-1,0} = gT^2_{m-1,0}/(2\pi)$ being the mean spectral wave length. The same three offshore wave steepness were tested in both HB and SF configurations. Table 1 reports also two important non-dimensional parameters, the relative water depth h_t/H_{m0} and the relative crest wall freeboard R_c/H_{m0}. While the HB tests have been performed to cover wide range of the parameter $h_t/H_{m0,t}$, the SF tests

Table 1
List of hydraulic and geometrical parameter ranges.

Parameter		HB (35 tests)	SF (112 tests)
$cot(\Theta)$	[–]	∞	50
h_t	m	0.30 ÷ 0.80	0.05 ÷ 0.30
R_c	m	0.10; 0.20	0.10 ÷ 0.75
$H_{m0,o}$	m	–	0.07 ÷ 0.17
$T_{m-1,0,o}$	s	–	1.16 ÷ 3.05;
$s_{m-1,0,o}$	[–]	–	0.01; ÷ 0.06
$H_{m0,t}$	m	0.075 ÷ 0.105	0.053 ÷ 0.142
$T_{m-1,0,t}$	s	1.03 ÷ 2.43	1.16 ÷ 3.66;
$s_{m-1,0,t}$	[–]	0.009 ÷ 0.053	0.005 ÷ 0.04
$\frac{h_t}{H_{m0,t}}$	[–]	2.93 ÷ 10.66	0.71 ÷ 4.78
$\frac{R_c}{H_{m0,t}}$	[–]	0.96 ÷ 2.19	0.8 ÷ 6.3
q	[$m^3/s/m$]	$0 \div 2.34 \cdot 10^{-4}$	$0 \div 5.97 \cdot 10^{-4}$
q^*	[–]	$0 \div 2.76 \cdot 10^{-3}$	$0 \div 7.43 \cdot 10^{-3}$
N_w	[–]	791 ÷ 1000	782 ÷ 1000

were intended to further explore the impulsive overtopping for high value of the relative freeboard $R_c/H_{m0,t}$. The HB tests are almost in theoretically deep water conditions, i.e. $h_t/H_{m0,t} > 4$, except the tests with 0.3 m of water depth; while the SF tests are almost all in intermediate or shallow water conditions, except 6 tests with $h_t = 0.3$ m and the smaller $H_{m0,t}$, when $h_t/H_{m0,t} > 4$. In Table 1 are reported the ranges of measured mean overtopping discharges, q in $m^3/s/m$ and the non-dimensional mean overtopping discharge, q^*, obtained as defined by Eq. (5) later in Section 3.1.

In SF tests the water depth at wave-maker, h_o, is 0.41 m deeper than h_t, therefore, in order to ensure a good wave generation ($h_o \geq 3H_{m0,o}$) only the wave height $H_{m0,o} = 0.10$ m was tested for the shallower water tests (with $h_t \leq 0.10$ m).

The values in Table 1 represent the incident wave conditions obtained by the wave gauges array measurements according to the method proposed by Røge Eldrup and Lykke Andersen (2019) for separation of incident and reflected waves. The proposed model study for the SF configuration is performed on a foreshore 10.5 m long, excluding the transition slope, therefore longer of at least two times the local wave length. Wolters et al. (2010), in HYDRALAB guidelines, indeed recommend a foreshore length of 3–5 times the local wave length, to model wave shoaling and breaking accurately. However, the overtopping results have been analyzed referring always to wave conditions at the toe of the wall. As explained later in Section 2.5, all the tested wave and level conditions at the toe of the wall have been measured during calibration tests.

For both campaigns the tests were carried out reproducing a JONSWAP spectrum (Hasselmann et al., 1973) with a duration of 1000 waves (2nd order wave generation); except when 1000 waves take more than 30 min, then a total duration of 30 min was adopted for those tests. For all the experiments at least 700 waves were generated, needed to obtain reliable wave overtopping results as stated by Romano et al. (2015) and Williams et al. (2019). In Table 1, N_w reports the ranges of the number of waves reproduced.

In order to perform tests for wide ranges of h_t and R_c, in the HB configuration a modular wall was used, made of several wall pieces, 0.1 m high (as can be noted from the pictures in Fig. 2), added for each test with a higher freeboard or in deeper water. Fig. A.12 in Appendix explains the wall set-up of the SF tests. Three walls have been used during these experiments, to get different freeboards during different water depth tests. For each test, the wall and the chute have been fixed at different vertical positions, as can be noted in Fig. 3.

2.5. Calibration tests for SF configuration

Given the presence of the 1:50 sloped foreshore, all the combinations of wave and water depth performed in the SF tests, have been previously modeled in the wave flume without the vertical wall, which

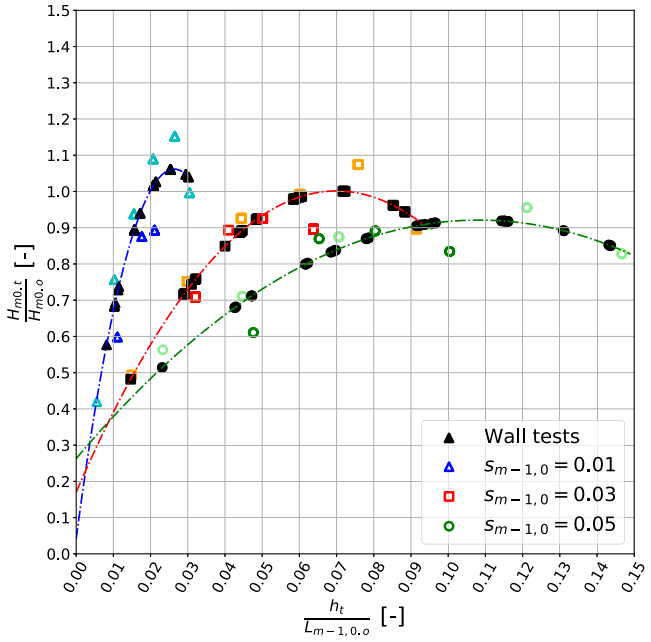

Fig. 4. Incident significant wave height ratios against the relative water depth. The data have been plotted separately based on the wave steepness: the triangles, the squares and the circles refers to $s_{m-1,0} = 0.01$, $s_{m-1,0} = 0.03$ and $s_{m-1,0} = 0.05$, respectively. Darker colors for $H_{m0,o} = 0.15$ m and lighter colors for $H_{m0,o} = 0.10$ m. The black markers refer to the SF tests with the wall in place.

was replaced by an array of three wave gauge. These calibration tests allowed in getting exclusively the incident wave condition at the toe of the wall, h_t, as suggested by Wolters et al. (2010) and Koosheh et al. (2021). Hence, during these tests, 3 wave gauges were installed in an offshore position, close to the wave-maker and other 3 at the toe of the structure, as can be noted from the sketch of Fig. 1(*b*). A passive wave absorber was placed at the flume's end opposite to the wave maker, during these calibration tests. The incident wave parameters offshore and at water depth h_t, have been calculated with the method proposed by Røge Eldrup and Lykke Andersen (2019) to separate incident and reflected waves.

For each calibration test a transformation factor was calculated as the ratio between the spectral wave height at the toe $H_{m0,t}$ and the offshore one $H_{m0,o}$. In Fig. 4 this ratio is plotted against $h_t/L_{m-1,0,o}$. The colored markers refer to the calibration test results (29 tests), differentiated for the three tested wave steepness, as indicated in the legend. The markers with darker colors are relative to tests with $H_{m0,o} = 0.15$ m, while the markers with lighter colors refer to tests with $H_{m0,o} = 0.10$ m. Three dashed curves (second degree polynomial) describe the relationship between the generated deep water wave height and the one at the toe of the structure. Indeed, the black colored markers, aligned with the curves, refer to all the SF tests with the wall in the wave flume.

Regarding the variation of the wave period from offshore to shallow water, although the peak period, T_p, remains almost constant, this is no longer valid for the spectral period $T_{m-1,0}$, which is influenced by low-frequency energy. Hofland et al. (2017) proposed an empirical model to predict this spectral wave period as a function of the relative water depth and the slope of the foreshore Θ:

$$\frac{T_{m-1,0,t}}{T_{m-1,0,o}} = 1 + 6exp(-4\widetilde{h}) + exp(-\widetilde{h}) \quad (1)$$

where $\widetilde{h}$ is defined as:

$$\widetilde{h} = \frac{h_t}{H_{m0,o}}\left(\frac{cot\Theta}{100}\right)^{0.2} \quad (2)$$

Eq. (1) is valid for mildly sloped foreshore, defined by:

$$\Theta T_{m-1,0,o}\sqrt{\frac{g}{H_{m0,o}}} < 0.62 \tag{3}$$

The SF tests respect the requirement of Eq. (3) and the calibration tests results confirm the applicability of Eq. (1). Therefore, in order to get the incident spectral wave period at the wall during the SF test, the relation (1) was adopted, knowing the offshore wave characteristics.

Therefore, these ad hoc calibration tests allowed to assess the variation of the wave characteristics from deeper to shallower water and to find the incident wave conditions at the wall, in the SF configuration. Then, during the SF tests with the wall installed, only the wave gauge array in the offshore position was left in the flume and the same wavemaker motion time series of the calibration tests were reproduced, even varying the wall crest freeboard for the same wave conditions. The significant wave height and spectral period at the toe of the wall have been related to the offshore measured wave, using the relations shown in Fig. 4 and by Eq. (1) respectively.

3. Analysis and results

A total of 147 tests (35 with HB configuration and 112 with SF configuration) were carried out. In the following, the mean overtopping discharge results are firstly presented, followed by the individual wave overtopping events analysis. The tests that measured a mean overtopping discharge less than 10^{-6} m^3/s/m have been removed from the following analysis, considering it as a limit of significant overtopping rate, as reported by Verhaeghe et al. (2008). A total of 116 tests were consequently analyzed (29 with HB configurations and 87 with SF configuration).

3.1. Average wave overtopping discharge results

As reported in EurOtop (2018) guidelines, for vertical structure a first distinction is made between impulsive and non-impulsive conditions. The method proposed within the PROVERBS project (Oumeraci et al., 2001), from the approach originally developed by Besley et al. (1998) and Pearson et al. (2001), makes use of a wave breaking parameter h^* determined from the water depth at the toe of the structure h_t and the incident wave conditions, as follows:

$$h^* = \frac{h_t^2}{H_{m0,t}L_{m-1,0,t}} \tag{4}$$

The impulsive conditions occurs when $h^* \leq 0.23$, while the non-impulsive when $h^* > 0.23$.

Among the HB tests, 33 out of 35 are non-impulsive, while 93 out of 112 SF tests are impulsive wave conditions.

Fig. 5 shows the test results under non-impulsive conditions for both configurations, squared and rounded markers respectively for HB and SF tests. The non-dimensional mean overtopping discharge q^*, in Fig. 5 is calculated as

$$q^* = \frac{q}{\sqrt{gH_{m0,t}^3}} \tag{5}$$

where q is the mean overtopping discharge in m^3/s/m.

Results are compared with the reference equations proposed by EurOtop (2018), which makes a further discrimination for the case of plain vertical walls: whether there is or not any influence of the foreshore.

For the case of vertical wall without foreshore influence the EurOtop (2018) proposes the 7.1 formula:

$$q^* = 0.047\exp\left[-\left(2.35\frac{R_c}{H_{m0}}\right)^{1.3}\right] \tag{6}$$

to relate the non-dimensional mean overtopping discharge (5) with the relative freeboard $R_c/H_{m0,t}$. Eq. (6) is displayed in Fig. 5 with a dashed line. Please note that among all the 35 HB tests, two of these were in impulsive conditions, in particular: one test for $h_t = 0.3$ m; $R_c = 0.2$ m; $H_{m0,t} = 0.1$; $T_{m-1,0,t} = 2.5$, and the second test for $h_t = 0.3$ m; $R_c = 0.1$ m; $H_{m0,t} = 0.1$; $T_{m-1,0,t} = 2.5$. However, these tests are reported in Fig. 5 since EurOtop (2018), for vertical walls without the influence of the foreshore, does not make distinction between non-impulsive and impulsive conditions and the mean overtopping discharge is estimated with Eq. (6). These two tests are reported with black square markers in Fig. 5.

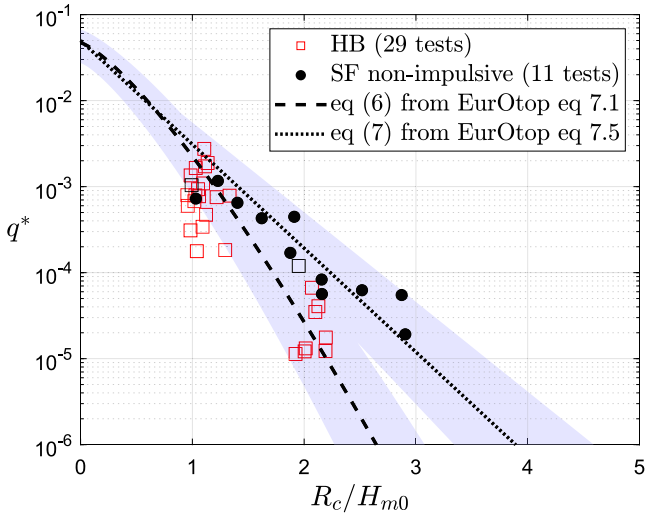

Fig. 5. Results of measured wave overtopping non-dimensional average discharges under non-impulsive conditions, for HB tests (squares) and for SF tests (circles). The dashed line reports the 7.1 Eurotop formula (Eq. (6)) for vertical wall not influenced by the foreshore; the dotted line reports the 7.5 Eurotop formula (Eq. (7)) for vertical wall with influence of the foreshore and under non-impulsive conditions.

Conversely, when there is a foreshore influence, under non-impulsive conditions the mean overtopping discharge can be predicted by using the equation originally proposed by Allsop (1995) in conditions of shallower water, and reported in EurOtop (2018) as 7.5 formula, that reads as:

$$q^* = 0.05\exp\left(-2.78\frac{R_c}{H_{m0}}\right) \tag{7}$$

Eq. (7) is also reported in Fig. 5 with a dotted line. In Fig. 5 the shaded areas around the lines representing the Eurotop predictions are the 5% exceeding lines (or 90% confidence bands). To quantitatively evaluate the fitting of the experimental data with the EurOtop (2018) formulas, for non-impulsive conditions, Table 2 reports the accuracy metrics, so defined:

$$BIAS = \frac{1}{n}\sum_{i=1}^{n}\left[log\left(q^*_{pred_i}\right) - log\left(q^*_{meas_i}\right)\right] \tag{8}$$

$$RMSE = \sqrt{\frac{1}{n}\sum_{i=1}^{n}\left\{\left[log\left(q^*_{pred_i}\right) - log\left(q^*_{meas_i}\right)\right]^2\right\}} \tag{9}$$

$BIAS$ can be both positive (overall over prediction) or negative (overall under prediction). The root mean-square error ($RMSE$) is always non-negative and it is zero for perfect prediction. The same metrics have been used also to compare the experimental data with the formulas proposed by Shaeri and Etemad-Shahidi (2021).

The measured mean overtopping discharge under impulsive conditions for the remaining 76 SF tests are presented in Fig. 6. Here, the mean overtopping discharge reads as Q^*, is calculated as

$$Q^* = \frac{q}{\sqrt{gH_{m0}^3}\sqrt{\frac{H_{m0}}{h_t s_{m-1,0,t}}}} \tag{10}$$

Table 2
Performance comparison of non-impulsive tests with EurOtop (2018) and Shaeri and Etemad-Shahidi (2021) formulas.

	EurOtop (2018)	Shaeri and Etemad-Shahidi (2021)
BIAS	0.158	0.570
RMSE	0.416	0.728

Table 3
Performance comparison of impulsive tests with EurOtop (2018) and Shaeri and Etemad-Shahidi (2021) formulas.

	EurOtop (2018)	Shaeri and Etemad-Shahidi (2021)
BIAS	0.481	0.210
RMSE	0.651	0.507

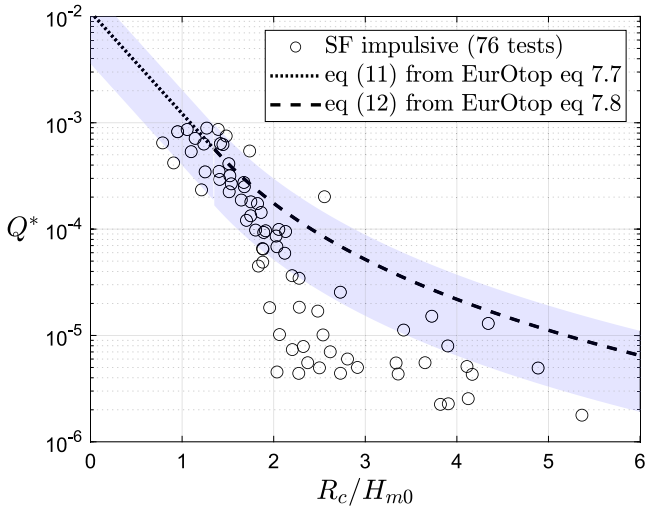

Fig. 6. Results of measured wave overtopping non-dimensional average discharges under impulsive conditions for SF tests. The dotted and dashed lines report respectively the Eurotop formula 7.7 (Eq. (11)) and 7.8 (Eq. (12)), which are valid for vertical wall influenced by the foreshore under impulsive wave conditions.

as suggested by the EurOtop (2018). From the literature, the mean overtopping discharge under impulsive conditions are described by two formulae as stated by Van der Meer and Bruce (2014) and reported in EurOtop (2018): an exponential equation for lower freeboards, and a power-law equation for the higher freeboards, which state as:

$$Q^* = 0.011 \exp\left(-2.2\frac{R_c}{H_{m0}}\right) \quad \text{for} \quad 0 < \frac{R_c}{H_{m0}} < 1.35 \tag{11}$$

$$Q^* = 0.0014\left(\frac{R_c}{H_{m0}}\right)^{-3} \quad \text{for} \quad R_c/H_{m0} \geq 1.35 \tag{12}$$

These two formulas (Eqs. (11) and (12)) are shown in Fig. 6 respectively with a dotted and dashed lines, while the shaded areas represent their relative 90% band of confidence. The few tests carried out with a relative freeboard lower that 1.35, fit well with the EurOtop (2018) prediction formula (Eq. (11)); while the tests performed with higher relative freeboards would be overestimated by Eq. (12). To quantify the accuracy of the prediction, Table 3, as Table 2, reports the values for the metrics defined in Eqs. (8) and (9).

As expected, the experimental data, especially for higher freeboards are better predicted by Shaeri and Etemad-Shahidi (2021) formulas, which have a range of applicability up to 5.24 for the relative cres freeboard. EurOtop (2018) instead proposed Eq. (12) based on fitting laboratory data performed exclusively with $\frac{R_c}{H_{m0}}$ lower than 3.3.

The new tests suggest more an exponential behavior of Q^* with the relative freeboard, even for larger values of R_c/H_{m0}. Moreover, the foreshore slope influences the mean overtopping discharge, as stated by Shaeri and Etemad-Shahidi (2021), when $h_t/H_{mo,t} < 3$. Further investigations are therefore ongoing within the WOW project testing different slopes of the foreshore.

3.2. Individual wave overtopping discharge results

As stated in the introduction, it is now recognized that individual volumes of wave overtopping are important, when analyzing the hydraulic performances of a structure. Therefore, in the last years a considerable research effort is made to describe the probability distribution of individual overtopping volumes. These two new experimental datasets allow to further investigate on this topic. In the HB configuration, the wave overtopping measurement is obtained from the water level time series inside the overtopping tank, recorded by a wave gauge. The original signal was filtered using a low pass digital filter (f_{cutoff} = 0.5 Hz). During the HB test the timing of each overtopping event has been registered, allowing to get the time of its occurrence in the wave gauge signal. Then, the mean value of the filtered signal between two consecutive overtopping events has been considered and multiplied by the surface area of the tank to get the individual overtopping volumes.

In the SF configuration, the wave overtopping measurement is given by a dynamo-meter that reports the overtopped water weight time series, further converted in water volume time series. No robust techniques are reported for the identification of the individual overtopping event (Koosheh et al., 2021). In this campaign, the derivative of the cumulative volumes curve is applied to each test and then a threshold has been set to determine the single event. This approach is based on the assumption that when there are no overtopping events the cumulative curve is a horizontal line; on the other hand, when an increase occurs, the derivative is positive. The threshold value for the derivative was established at 0.0002, through a process of trial and error, based on both visual observations during the physical tests and post-processing analysis of the time series data and videos. This iterative approach allowed us to identify a value that effectively captures significant changes in the signal. These measurements allowed to define for each test, the individual volumes, the maximum volume V_{max} and the number of overtopping events N_{ow}. Therefore, the proportion of overtopping waves, P_{ov}, can be defined as the ratio of the number of overtopping events over the number of incident waves. As stated in EurOtop (2018), a correlation has been noted between the proportion of overtopping waves with the relative freeboards R_c/H_{m0}, for vertical structures. In particular, it is stated that for non-impulsive condition the relation (Franco et al., 1994) is valid:

$$\frac{N_{ow}}{N_w} = exp\left[-1.2\left(\frac{R_c}{H_{m0}}\right)^2\right] \tag{13}$$

while under impulsive condition, N_{ow} is given by (Besley et al., 1998):

$$\frac{N_{ow}}{N_w} = \max\begin{cases}\exp\left[-1.2\left(\frac{R_c}{H_{m0}}\right)^2\right] \\ 0.024\left(h^*\frac{R_c}{H_{m0}}\right)^{-1}\end{cases} \tag{14}$$

The experimental data from both HB and SF configurations are reported in the same Fig. 7 in terms of proportion of overtopping waves with the relative freeboards. The SF test results are marked with black filled circles for non-impulsive conditions and with white filled circles for impulsive conditions; red squared markers refer to the HB test results. Fig. 7 also reports the EurOtop (2018) formulas: the continuous black line refers to Eq. (13) and it is valid for non impulsive conditions; the gray dashed lines refer to Eq. (14), applicable for impulsive conditions with three different values of h^*. The new experimental dataset shows a behavior similar to that indicated by the EurOtop (2018), however a large variability can be noted, both for non impulsive and impulsive conditions. As highlighted in the work of Koosheh et al. (2021) for vertical wall under non impulsive condition

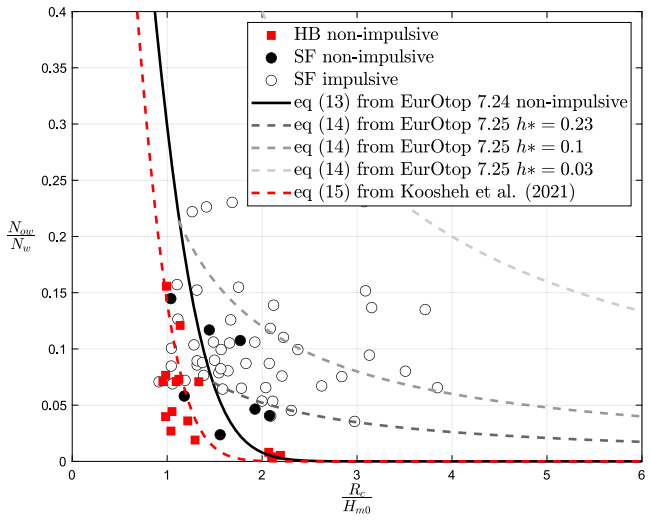

Fig. 7. Proportion of waves overtopping: non-impulsive and impulsive tests (only tests with $N_{ow} > 10$ are plotted), compared with existing formulae.

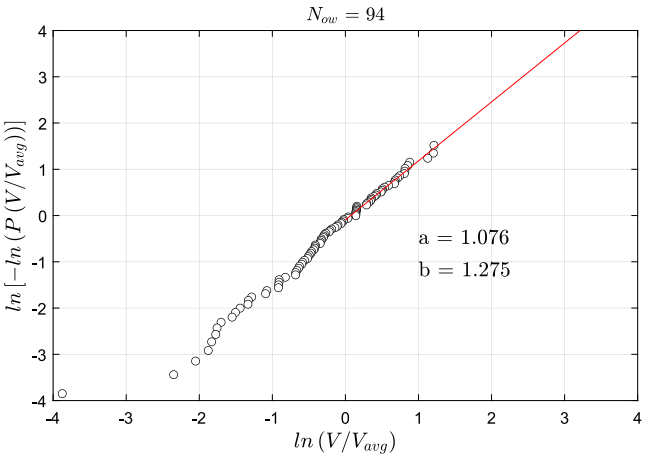

Fig. 8. Weibull plot of overtopping volumes for a test carried out in SF configuration, for impulsive conditions, with h_t = 0.15 m, $H_{m0,o}$ = 0.16, $s_{m-1,0,o}$ = 0.03 and R_c = 0.225 m.

the formula of Franco et al. (1994), gives slightly higher overtopping probabilities in comparison to the theoretical curve, which states that:

$$\frac{N_{ow}}{N_w} = exp\left[-\left(\frac{1}{\chi}\frac{R_c}{H_{m0}}\right)^2\right] \tag{15}$$

with $\chi = 0.708$. This curve is reported in Fig. 7 with a dashed red line.

The measurement of individual overtopping volumes during the model tests enabled the determination of their probability distribution. The distribution of individual overtopping volumes in a sequence is generally well described by a two-parameter Weibull distribution that states:

$$P(V_i \geq V) = exp\left[-\left(\frac{V}{a}\right)^b\right] \tag{16}$$

where P is the probability that an individual overtopping volume V_i will exceed a specified volume V. The two parameters of the Weibull distribution are the non-dimensional shape factor, b, and the dimensional scale factor, a, that normalizes the distribution. The shape parameter b represents the degree of concavity of the curve of the probability distribution. Generally, for a given average overtopping discharge, low values of the shape parameter indicate a high probability of having very large maximum volumes. When b becomes larger, the average overtopping rate is formed by more similar individual volumes as the volumes are more equally distributed. The scale factor a depends on the mean overtopping discharge, in particular large values of individual volumes correspond to larger values of the factor a.

By focusing exclusively on tests where the number of overtopping waves N_{ow} exceeded 10 (to ensure statistical significance), the exceeding empirical frequency was computed as function of the total number of overtopping waves N_{ow} (Su et al., 1992; Goda, 2010) as:

$$P'(V/V_{avg}) = \frac{i}{N_{ow}+1} \tag{17}$$

where the factor i represents the rank of the individual volumes, ranked in descending order, and P' is the empirical exceeding frequency of the normalized volumes, where V_{avg} is the average overtopping volume of each test. The empirical frequency of each individual volume for a single test, taken as example, is shown in a Weibull plot on Fig. 8. The test is relative to SF configuration with h_t = 0.15 m, $H_{m0,o}$ = 0.16, $s_{m-1,0,o}$ = 0.03 and R_c = 0.225 m.

It has been noted that the two-parameter Weibull distribution is a good fit particularly at higher values of the individual volumes, and that the contribution of small overtopping volumes in many cases deviates from the upper part, i.e. larger volumes, of the distribution (Victor et al., 2012; Zanuttigh et al., 2013; Salauddin et al., 2022). Therefore, the fitting of the individual volumes has been done only among volumes larger than V_{avg}, as can be noted by the straight red line in Fig. 8. Hence, the a and b factors were determined from the slope and from the y-intercept of the straight line that best fit the volumes larger than V_{avg}.

Assuming a Weibull probability distribution of the individual overtopping volumes, the scientific community sought for an empirical estimation of the scale and shape parameters, a and b, in order to estimate the probability distribution and the maximum individual volume for different wave and structure characteristics. Koosheh et al. (2021) review the basic concepts of the individual wave overtopping analysis, both for sloped and vertical coastal structures. For vertical structures, the shape factor b proposed by Franco et al. (1994) and Franco and Franco (1999) is 0.75. Later EurOtop (2018) indicates for non-impulsive conditions b = 0.66 for $s_{m-1,0}$ = 0.02 and b = 0.82 for $s_{m-1,0}$ = 0.04, while for impulsive conditions the b value becomes 0.85. To estimate the scale factor a (EurOtop, 2018) recommended the relationship:

$$a = \frac{1}{\Gamma(1+1/b)} * \frac{qT_m}{P_{ow}} \tag{18}$$

as obtained assuming that the theoretical V_{avg} is equal to $\frac{qT_m}{P_{ow}}$, where q is the mean overtopping discharge in $m^3/m/s$, T_m is the mean wave period obtained as $0.88T_{m-1,0}$ (EurOtop, 2018); P_{ow} is the probability of overtopping wave for a specific condition. To estimate the maximum individual volume Eq. (17) can be used, by obtaining P' with $i = 1$ and inverting Eq. (16) with $P = P'$ to get:

$$V_{max} = a\left[ln\left(N_{ow}\right)\right]^{1/b} \tag{19}$$

Lykke Andersen et al. (2009) pointed out that if N_{ow} is set to 1 in Eq. (19) the V_{max} is equal to 0. In order to have a more reliable evaluation of the maximum individual wave overtopping volume they suggested to use Eq. (19) with $\left(N_{ow}+1\right)$ as argument of the natural logarithm.

Therefore, the maximum individual volumes measured in HB and SF experimental campaigns have been compared with values of V_{max} predicted using Eq. (19). In particular, the value $b = 0.75$ has been assumed for non-impulsive conditions and b = 0.85 for impulsive conditions, and a has been calculated from Eq. (18). Fig. 9 shows this comparison between measured and predicted values. It can be noted that, a quite good prediction for small overtopping volumes, while for larger ones, under impulsive conditions the predicted maximum volumes are

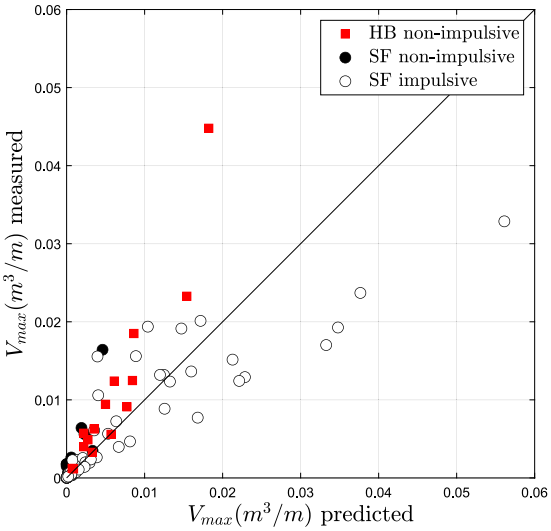

Fig. 9. Maximum individual volume of each test; comparison between measured values and predicted ones using Eq. (19).

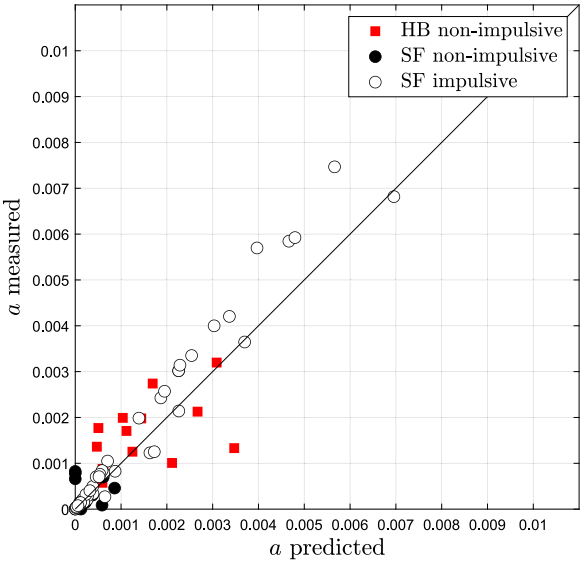

Fig. 10. Scale factor a of Weibull distribution; comparison of values obtained by fitting the experimental data and values given by Eq. (18) from EurOtop (2018).

overestimated, while in non-impulsive conditions the predicted values of V_{max} are underestimated. Therefore, to further investigate on this variability, i.e. $R^2 = 0.468$, the measured and predicted scale and shape parameters have been compared, given that the Weibull curve well describes the measured probability distribution of the individual overtopping volumes.

In Fig. 10 the values of a fitted by the present experimental campaigns (a measured) are compared to the theoretical ones (a predicted), obtained using Eq. (18), with the measured values of q and P_{ow} and the derived values of T_m at the toe of the wall, and assuming $b = 0.75$ for non-impulsive conditions and $b = 0.85$ for impulsive conditions. The data are quite well aligned with the bisector black line, i.e. $R^2 = 0.797$.

Since the value of the a parameter is estimated given the value of b parameter, in order to get a precise estimation of V_{max} an accurate prediction of Weibull shape factor, b, is needed. The amount of performed tests allows to investigate on the behavior of b values with the main wave and structure parameters. The fitted values of the shape

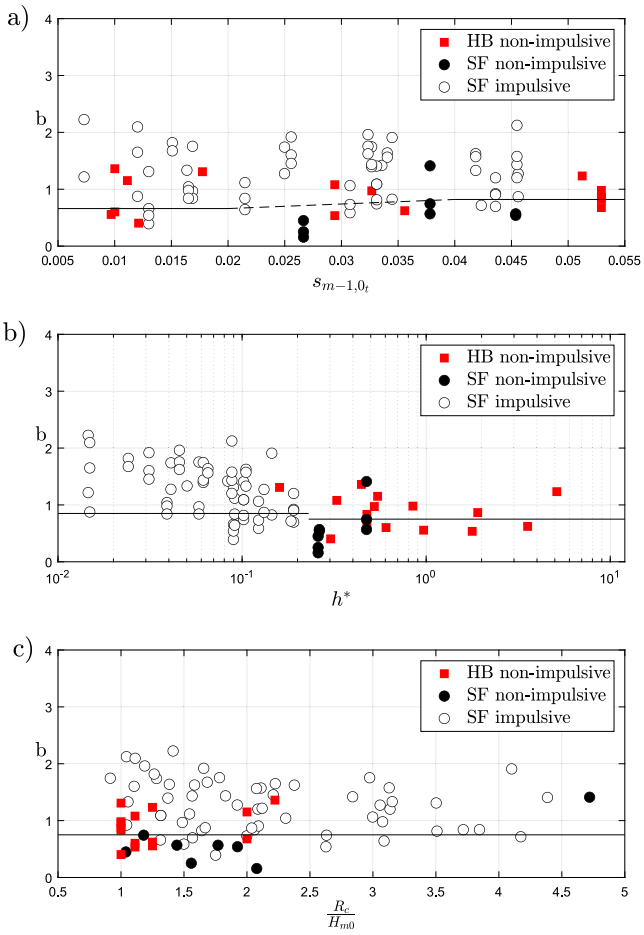

Fig. 11. Shape factor b of Weibull distribution against the wave steepness (a), relative water depth h^* (b) and relative freeboard (c); comparison with EurOtop formulae.

parameter b, are shown in Fig. 11 as function of the wave steepness, the relative freeboard and the relative water depth.

Fig. 11(a) highlights scatter in the data points, signifying no clear influence of wave steepness on the shape of the Weibull distribution, as already suggested by Salauddin et al. (2022). The continuous black lines in panel (a) indicate the suggested (EurOtop, 2018) constant values of b, equals to 0.66 for $s_{m-1,0_t} = 0.02$ and 0.82 for $s_{m-1,0_t} = 0.04$. In Fig. 11(b) it is shown the dependence of the b parameter with the relative water depth h^*, defined by Eq. (4). The two black lines represent the EurOtop (2018) values of 0.85 for $h^* \leq 0.23$ (impulsive) and of 0.75 for $h^* > 0.23$ (non-impulsive). It has to be noted that only in panel (b) the x-axis values are in a logarithmic scale, suggesting therefore, especially for impulsive conditions, an exponential behavior of b with the relative water depth. It can be observed that as wave–wall conditions become more impulsive, the values of the shape parameter b increase, indicating that under impulsive conditions, overtopping is characterized by numerous relatively small or limited wave volumes. This behavior was confirmed during the experimental tests observation. No particular dependence on the relative freeboard can be noted in panel (c), neither if just considering the individual volumes in the not yet fully explored range of R_c/H_{m0} larger than 3.3. The black line reports the value of 0.75 for the b parameter, that could be a valid estimate for non-impulsive conditions, more than for impulsive ones.

4. Conclusions

The purpose of this study was to investigate the wave overtopping at vertical structures under non-impulsive and impulsive conditions. A

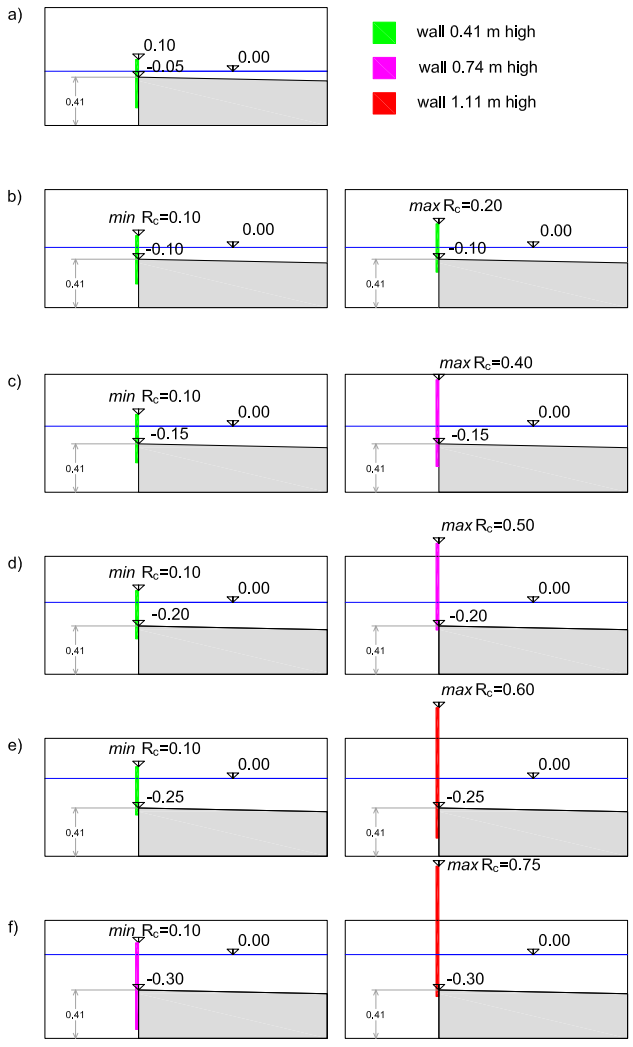

Fig. A.12. Experimental set-up of the SF tests. Sketches of the vertical walls positions for tests with different water depth at toe: (a) h_t = 0.05; (b) h_t = 0.10; (c) h_t = 0.15; (d) h_t = 0.20; (e) h_t = 0.25 and (f) h_t = 0.30. The left and right columns of plots are relative to the minimum and maximum freeboard tested respectively. The three walls are differently colored to test all the configurations: green wall is 0.41 high, the magenta one is 0.74 m high and the red one is 1.11 m high.

total number of 147 tests were carried out at the Roma Tre wave flume. Among these, 35 were tested over an horizontal sea-bottom, (HB configuration), and the remaining 112 were tested including a foreshore with a 1:50 slope, (SF configuration). Wave overtopping individual volumes were measured and the total volume of each test was used to calculate the average overtopping discharge. The proposed physical models are designed to be representative, in Froude similarity, of a quite broad range of vertical breakwater configurations, rather than replicating a specific existing structure. Nevertheless, a scale factor of approximately 1:50 is assumed. Although these laboratory experiments are conducted in small scale, Pearson et al. (2003) results show no significant difference in small and large scale overtopping, demonstrating that guidance from small-scale studies can be confidently applied to predict overtopping in prototype situations.

The experimental test results were compared with the prediction formulas from the EurOtop (2018). The measured mean overtopping discharges in non-impulsive condition resulted well estimated by EurOtop (2018) formulas, both in the case of no influence of the foreshore, i.e. Eq. (6), than in case of foreshore influence, i.e. Eq. (7). Regarding the measured overtopping discharges under impulsive conditions, a good agreement with Eq. (11) for low relative freeboard (R_c/H_{m0} < 1.35) it is found. For higher relative freeboard (R_c/H_{m0} > 1.35) the EurOtop formula reported in Eq. (12) (only limited to R_c/H_{m0} <3.3) overestimates the laboratory results. These experimental new data for relative freeboards also higher than 3.3 allow to investigate further on violent wave overtopping. It is undoubted that as the relative freeboard increases the overtopping discharge becomes lower, however, it is also well know that uncertainty on the overtopping discharge increases for high values of relative freeboards. Moreover, the foreshore plays a relevant role in wave transformation during propagation. Therefore, especially for impulsive condition, it is necessary to account for the influence of the foreshore when quantifying overtopping events. Although the EurOtop (2018) does not provide a specific relationship for foreshore slope, Shaeri and Etemad-Shahidi (2021) suggest that, consistent with the results of the presented tests, a flatter foreshore slope leads to a lower overtopping rate. Additionally, it should be noted that in real-world situations, the presence of wind significantly alters the nature of the overtopping hazard (van Gent et al., 2024).

This study, providing further wave by wave results, confirms the efficacy of the two-parameter Weibull distribution for modeling extreme overtopping volumes. The accurate estimation of the Weibull shape parameter b, is essential to estimate the individual volumes distributions and estimate the maximum volume. From the literature, for vertical structures the b parameter has been estimated constant, however, the proposed new tests show values of b with a variability in the range of 0.5–2. A similar range of variability has been found by Salauddin et al. (2022). No clear dependency of b value from the wave steepness neither from the relative freeboard can be noted. These tests are, among the fewest in literature, that investigate further on individual overtopping distribution for impulsive conditions. In particular, a decreasing exponential behavior of b values with the relative water depth can be noted. An underestimation of b induces an overestimation of the predicted maximum volumes, as can be noted in Fig. 9. These study findings suggest that the impulsiveness parameter plays a role on the distribution of wave-by-wave overtopping volumes at plain vertical walls.

Finally, it is worth to stress that, due to the complexity of the phenomena that take place, further research would be valuable. Specifically, it would be useful to consider also different values of the foreshore slope in the extended range of high relative freeboard, as already planned within WOW project.

CRediT authorship contribution statement

Claudia Cecioni: Writing – review & editing, Writing – original draft, Investigation, Data curation, Conceptualization, Formal analysis. **Yuri Pepi:** Writing – review & editing, Investigation, Data curation, Formal analysis. **Leopoldo Franco:** Writing – review & editing, Methodology, Conceptualization, Supervision.

Declaration of competing interest

The authors declare that they have no known competing financial interests or personal relationships that could have appeared to influence the work reported in this paper.

Acknowledgment

Authors gratefully acknowledge Prof. Jentsje Van der Meer and Prof. Tom Bruce for the organization of the WOW research project and for the fruitful discussions and their contribution to the on-going investigation of the wave data. Dr. Stefano de Finis and Dr. Verdiana Iorio are warmly acknowledged for their support during laboratory tests.

Appendix. Experimental set-up of SF configuration tests

See Fig. A.12.

Data availability

Data will be made available on request.

References

Akbari, H., 2017. Simulation of wave overtopping using an improved sph method. Coast. Eng. 126, 51–68.

Allsop, N., 1995. Overtopping performance of vertical and composite breakwaters, seawalls and low reflection alternatives. In: Paper To Final MAST-MCS Project Workshop, Alderney, UK, 1995. University of Hannover.

Altomare, C., Suzuki, T., Chen, X., Verwaest, T., Kortenhaus, A., 2016. Wave overtopping of sea dikes with very shallow foreshores. Coast. Eng. 116, 236–257.

Andersen, T.L., Clavero, M., Eldrup, M.R., Frigaard, P.B., Losada, M., 2018. Active absorption of nonlinear irregular waves. In: Coastal Engineering 2018. Coastal Engineering Research Council.

Andersen, T.L., Eldrup, M.R., Frigaard, P., 2017. Estimation of incident and reflected components in highly nonlinear regular waves. Coast. Eng. 119, 51–64.

AW, T., 2002. Technical Report. Technical Advisory Committee on Flood Defence.

Besley, P., 1999. Wave Overtopping of Seawalls, Design and Assessment Manual. R & D technical report W178.

Besley, P., Stewart, T., Allsop, N., 1998. Overtopping of vertical structures: New prediction methods to account for shallow water conditions. In: Proc. Int. Conf. on Coastlines, Structures and Breakwaters 1998. London, UK, pp. 46–57.

den Bieman, J.P., Van Gent, M.R., Van den Boogaard, H.F., 2021. Wave overtopping predictions using an advanced machine learning technique. Coast. Eng. 166, 103830.

Briganti, R., Musumeci, R.E., Van der Meer, J., Romano, A., Stancanelli, L.M., Kudella, M., Akbar, R., Mukhdiar, R., Altomare, C., Suzuki, T., et al., 2022. Wave overtopping at near-vertical seawalls: Influence of foreshore evolution during storms. Ocean Eng. 261, 112024.

Bruce, T., van der Meer, J., Pullen, T., Allsop, W., 2010. Wave overtopping at vertical and steep structures. In: Handbook of Coastal and Ocean Engineering. World Scientific, pp. 411–439.

De Rouck, J., Verhaeghe, H., Geeraerts, J., 2009. Crest level assessment of coastal structures—General overview. Coast. Eng. 56, 99–107.

EAK, 2002. Empfehlungen des Arbeitsausschusses Küstenschutzwerke. vol. 65, Empfehlungen für Küstenschutzwerke (EAK), Die Küste, H., (in German).

Etemad-Shahidi, A., Shaeri, S., Jafari, E., 2016. Prediction of wave overtopping at vertical structures. Coast. Eng. 109, 42–52.

EurOtop, 2007. In: Pullen, T., Allsop, N.W.H., Bruce, T., Kortenhaus, A., Schüttrumpf, H., Van der Meer, J.W. (Eds.), Wave Overtopping of Sea Defences and Related Structures: Assessment Manual.

EurOtop, 2018. In: Van der Meer, J., Allsop, N., Bruce, T., De Rouck, J., Kortenhaus, A., Pullen, T., Schüttrumpf, H., Troch, P., Zanuttigh, B. (Eds.), Manual on Wave Overtopping of Sea Defences and Related Sturctures: An Overtopping Manual Largely Based on European Research, But for Worlwide Application.

Franco, L., Bruce, T., Cecioni, C., Pepi, Y., Van der Meer, J., 2022. Violent and impulsive wave overtopping at vertical walls with large freeboards. Coast. Eng. Proc. 4, 0–40.

Franco, L., De Gerloni, M., Van der Meer, J., 1994. Wave overtopping on vertical and composite breakwaters. In: Coastal Engineering 1994. pp. 1030–1045.

Franco, C., Franco, L., 1999. Overtopping formulas for caisson breakwaters with nonbreaking 3d waves. J. Waterw. Port Coast. Ocean Eng. 125, 98–108.

Gallach-Sánchez, D., Troch, P., Kortenhaus, A., 2021. A new average wave overtopping prediction formula with improved accuracy for smooth steep low-crested structures. Coast. Eng. 163, 103800.

Goda, Y., 2009. Derivation of unified wave overtopping formulas for seawalls with smooth, impermeable surfaces based on selected clash datasets. Coast. Eng. 56, 385–399.

Goda, Y., 2010. Random Seas and Design of Maritime Structures. vol. 33, World Scientific Publishing Company.

Goda, Y., Kishara, Y., Kamiyama, Y., 1975. Laboratory Investigation on the Overtopping Rate of Seawalls By Irregular Waves. vol. 14, Report of the Port and Harbour Research Institute, nr. 4.

Hasselmann, K.F., Barnett, T.P., Bouws, E., Carlson, H., Cartwright, D.E., Eake, K., Euring, J., Gicnapp, A., Hasselmann, D., Kruseman, P., et al., 1973. Measurements of wind-wave growth and swell decay during the joint north sea wave project (jonswap). Ergaenzungsheft Dtsch. Hydrogr. Eitschrift, Reihe A.

Herbert, D., 1993. Wave Overtopping of Vertical Walls. HR Wallingford Report SR 316.

Hofland, B., Chen, X., Altomare, C., Oosterlo, P., 2017. Prediction formula for the spectral wave period $T_{m-1,0}$ on mildly sloping shallow foreshores. Coast. Eng. 123, 21–28.

Hu, K., Mingham, C.G., Causon, D.M., 2000. Numerical simulation of wave overtopping of coastal structures using the non-linear shallow water equations. Coast. Eng. 41, 433–465.

Hughes, S.A., 1993. Physical Models and Laboratory Techniques in Coastal Engineering, vol. 7, World Scientific.

Koosheh, A., Etemad-Shahidi, A., Cartwright, N., Tomlinson, R., van Gent, M.R., 2021. Individual wave overtopping at coastal structures: A critical review and the existing challenges. Appl. Ocean Res. 106, 102476.

Lashley, C.H., Van Der Meer, J., Bricker, J.D., Altomare, C., Suzuki, T., Hirayama, K., 2021. Formulating wave overtopping at vertical and sloping structures with shallow foreshores using deep-water wave characteristics. J. Waterw. Port Coast. Ocean Eng. 147, 04021036.

Losada, I.J., Lara, J.L., Guanche, R., Gonzalez-Ondina, J.M., 2008. Numerical analysis of wave overtopping of rubble mound breakwaters. Coast. Eng. 55, 47–62.

Lykke Andersen, T., Burcharth, H.F., Gironella, F., 2009. Single wave overtopping volumes and their travel distance for rubble mound breakwaters. In: Coastal Structures 2007. vol. 2, World Scientific, pp. 1241–1252.

Oumeraci, H., Kortenhaus, A., Allsop, W., de Groot, M., Crouch, R., Vrijling, H., Voortman, H., 2001. Probabilistic Design Tools for Vertical Breakwaters. CRC Press.

Owen, M., 1980. Design of seawalls allowing for wave overtopping. Rep. Ex 924 (39).

Pearson, J., Bruce, T., Allsop, W., 2001. Prediction of wave overtopping at steep seawalls—Variabilities and uncertainties. In: Ocean Wave Measurement and Analysis (2001). pp. 1797–1808.

Pearson, J., Bruce, T., Allsop, W., Gironella, X., 2003. Violent wave overtopping–measurements at large and small scale. In: Coastal Engineering 2002: Solving Coastal Conundrums. World Scientific, pp. 2227–2238.

Røge Eldrup, M., Lykke Andersen, T., 2019. Estimation of incident and reflected wave trains in highly nonlinear two-dimensional irregular waves. J. Waterw. Port Coast. Ocean Eng. 145, 04018038.

Romano, A., Bellotti, G., Briganti, R., Franco, L., 2015. Uncertainties in the physical modelling of the wave overtopping over a rubble mound breakwater: The role of the seeding number and of the test duration. Coast. Eng. 103, 15–21.

Salauddin, M., O'Sullivan, J., Abolfathi, S., Peng, Z., Dong, S., Pearson, J.M., 2022. New insights in the probability distributions of wave-by-wave overtopping volumes at vertical breakwaters. Sci. Rep. 12 (16228).

Salauddin, M., Pearson, J.M., 2019. Wave overtopping and toe scouring at a plain vertical seawall with shingle foreshore: A physical model study. Ocean Eng. 171, 286–299.

Shaeri, S., Etemad-Shahidi, A., 2021. Wave overtopping at vertical and battered smooth impermeable structures. Coast. Eng. 166, 103889.

Su, J., Liu, C., Kuo, C., 1992. Application of weibull distribution for irregular wave overtopping. In: Proc. of 6th IAHR Symp. on Stochastic Hyd. Taipei, Taiwan.

Suzuki, T., Altomare, C., Veale, W., Verwaest, T., Trouw, K., Troch, P., Zijlema, M., 2017. Efficient and robust wave overtopping estimation for impermeable coastal structures in shallow foreshores using swash. Coast. Eng. 122, 108–123.

USACE, 2002. Coastal Engineering Manual. CEM, U.S. Army Corps of Engineers, Vicksburg, Mississipi, USA.

Van der Meer, J., Bruce, T., 2014. New physical insights and design formulas on wave overtopping at sloping and vertical structures. J. Waterw. Port Coast. Ocean Eng. 140, 04014025.

Van der Meer, J., Janssen, J., 1994. Wave Run-Up and Wave Overtopping At Dikes. technical report, vol. 485, Delft Hydraulics, Delft.

Van der Meer, J.W., Verhaeghe, H., Steendam, G.J., 2009. The new wave overtopping database for coastal structures. Coast. Eng. 56, 108–120.

Van Gent, M.R., Van den Boogaard, H.F., Pozueta, B., Medina, J.R., 2007. Neural network modelling of wave overtopping at coastal structures. Coast. Eng. 54, 586–593.

Van Gent, M., Smith, G., 1999. Physical model investigations on coastal structures with shallow foreshores: 2d model tests with single and double-peaked wave energy spectra.

van Gent, M., van der Bijl, R., Wolters, G., Wüthrich, D., 2024. The maximum influence of wind on wave overtopping at seawalls with crest elements. In: Coasts, Marine Structures and Breakwaters 2023: Resilience and Adaptability in a Changing Climate. Emerald Publishing Limited, pp. 1007–1021.

Verhaeghe, H., De Rouck, J., van der Meer, J., 2008. Combined classifier–quantifier model: A 2-phases neural model for prediction of wave overtopping at coastal structures. Coast. Eng. 55, 357–374.

Victor, L., Troch, P., 2013. Experimental study on the overtopping behaviour of steep slopes: Transition between mild slopes and vertical walls. In: 33rd International Conferenc on Coastal Engineering. pp. 1–24.

Victor, L., Van der Meer, J., Troch, P., 2012. Probability distribution of individual wave overtopping volumes for smooth impermeable steep slopes with low crest freeboards. Coast. Eng. 64, 87–101.

Williams, H.E., Briganti, R., Romano, A., Dodd, N., 2019. Experimental analysis of wave overtopping: A new small scale laboratory dataset for the assessment of uncertainty for smooth sloped and vertical coastal structures. J. Mar. Sci. Eng. 7 (217).

Wolters, G., van Gent, M., Allsop, W., Hamm, L., Muhlestein, D., 2010. Hydralab iii: Guidelines for physical model testing of rubble mound breakwaters. In: Coasts, Marine Structures and Breakwaters: Adapting To Change: Proceedings of the 9th International Conference Organised By the Institution of Civil Engineers and Held in Edinburgh on 16 To 18 2009. Thomas Telford Ltd., pp. 559–670.

Zanuttigh, B., Formentin, S.M., van der Meer, J.W., 2016. Prediction of extreme and tolerable wave overtopping discharges through an advanced neural network. Ocean Eng. 127, 7–22.

Zanuttigh, B., van der Meer, J., Bruce, T., Hughes, S., 2013. Statistical characterisation of extreme overtopping wave volumes. In: From Sea To Shore–Meeting the Challenges of the Sea: (Coasts, Marine Structures and Breakwaters 2013). vol. 44, ICE Publishing, pp. 2–451.